LANGMUIR

Article

Reversible protein adsorption on mixed PEO/PAA polymer brushes – role of ionic strength and PEO content

Anna Bratek-Skicki, Pierre Eloy, Maria Morga, and Christine C. Dupont-Gillain

Langmuir, **Just Accepted Manuscript** • DOI: 10.1021/acs.langmuir.7b04179 • Publication Date (Web): 06 Feb 2018

Langmuir is published by the American Chemical Society. 1155 Sixteenth Street N.W., Washington, DC 20036

Reversible protein adsorption on mixed PEO/PAA polymer brushes – role of ionic strength and PEO content

Anna Bratek-Skicki*[1,2], Pierre Eloy[1], Maria Morga[2], Christine Dupont-Gillain*[1]

1- *Institute of Condensed Matter and Nanosciences, Université catholique de Louvain, Place Louis Pasteur (L4.01.10), 1348 Louvain-la-Neuve, Belgium*
2- *Jerzy Haber Institute of Catalysis and Surface Chemistry, Polish Academy of Sciences, Niezapominajek 8, PL30239 Krakow, Poland*

*Corresponding authors:

christine.dupont@uclouvain.be

ncbratek@cyf-kr.edu.pl

ABSTRACT

Proteins at interfaces are a key for many applications in the biomedical field, in biotechnologies, in biocatalysis, in food industry etc. The development of surface layers that allow to control and manipulate proteins is thus highly desired. In previous works, we have shown that mixed polymer brushes combining the protein-repellent properties of poly(ethylene oxide) (PEO) and the stimuli-responsive adsorption behavior of poly(acrylic acid) (PAA) could be synthesized and used to achieve switchable protein adsorption. With the present work, we bring more insight into the rational design of such smart thin films by unravelling the role of PEO on the adsorption/desorption of proteins. The PEO content of the mixed PEO/PAA brushes was regulated, on the one hand, by using PEO with different molar masses, and on the other hand, by varying the ratio of PEO and PAA in the solutions used to synthesize the brushes. The influence of ionic strength on the protein adsorption behavior was also further examined. The behavior of three proteins: human serum albumin, lysozyme and human fibrinogen, which have very different size, shape, and isoelectric point, was investigated. X-ray photoelectron spectroscopy, quartz crystal microbalance, atomic force microscopy and streaming potential measurements were used to characterize the mixed polymer brushes and, in particular, to estimate the fraction of each polymer within the brushes. Protein adsorption and desorption conditions were selected based on previous studies. While brushes with a lower PEO content allowed the higher protein adsorption to occur, fully reversible adsorption could only be achieved when the PEO surface density was at least 25 PEO units per nm^2. Taken together, the results increase the ability to finely tune protein adsorption, especially with temporal control. This opens up possibilities of applications in biosensor design, separation technologies, nanotransport etc.

KEYWORDS: protein adsorption, polymer brushes, PEO/PAA stimuli-responsive polymer brushes, quartz crystal microbalance, X-ray photoelectron spectroscopy, streaming potential

INTRODUCTION

Protein adsorption at solid/liquid interfaces is a common phenomenon that has received increasing attention due to its importance in the biomedical and biotechnology fields. Controlling protein adsorption is important for the development of biomedical applications, such as enzyme carriers, immunological tests, and drug delivery devices[1-4]. On the other hand, non-specific protein adsorption on sensor surfaces, protein chips, or assay platforms is a serious problem, regarding the analytical performances of the device[5]. Most proteins are large amphiphatic molecules, which makes them intrinsically surface active. A thermodynamic inventory of the various interactions that contribute to protein adsorption was made by Haynes and Norde[6]. The origin of these interactions is found in intermolecular forces, such as Coulombic, van der Waals, and Lewis acid-based forces, and more entropically-based effects such as hydrophobic interactions, conformational entropy and restricted mobility. Moreover, the adsorption process depends on intramolecular forces within the protein molecules, and may lead to alterations of protein conformation. As a result, one sometimes finds a large difference between protein adsorption and desorption behavior, leading to an apparent irreversibility of the adsorption process. It is therefore challenging to achieve a temporal control over protein adsorption.

Many strategies were recently developed to spatially or temporally control protein adsorption, most of them based on the use of polymers at interfaces. Protein adsorption may be tuned using smart interfaces based on stimuli-responsive polymer brushes. These systems are promising for numerous important applications due to their ability to switch interaction forces between the brush chains and the surrounding environment. The polymer conformation can be tuned by a variety of external stimuli such as temperature, electric or magnetic fields, salt concentration and/or pH of the solution. Polyelectrolyte brushes have been intensively studied for their swelling behavior. The weak polyelectrolyte brushes are especially auspicious because their properties, including surface wettability or electrostatic interactions, can be switched according to changes in pH, ionic strength, valence of counterions, and grafting density[7,8].

Polyanionic brushes consisting of poly(acrylic acid) (PAA) are widely studied for their pH-dependent deprotonation of COOH groups and their non-monotonic swelling depending on the ionic strength I of the solution[9,10]. The interaction range is characterized by the Debye screening length κ^{-1} which depends on the salt concentration of the bulk solution. Hence, the brush profile varies with changes in the ionic strength. The swelling of the brush is driven by osmotic pressure,

caused by the presence of counterions inside the polymer brush. In the osmotic regime, an increase of the ionic strength leads to an increase of counterion condensation inside the brush. Further increase of the ionic strength decreases the Debye screening length. The brush enters the salted regime and collapses[11-12]. In previous works[13-15] it was shown that protein adsorption decreased on collapsed PAA brushes. When the brushes are swollen, proteins may enter inside the brush, leading to high adsorbed amounts. Haupt et al.[16] immobilized glucoamylase and β-glucosidase into brushes of PAA or poly(styrene sulfonic acid) (PSS) grafted on spherical polystyrene beads. The activity of these immobilized enzymes was largely preserved, whereas the Michaelis constant decreased with increased amounts of immobilized enzymes. Poly(ethylene oxide) (PEO), also known as poly(ethylene glycol) (PEG), molecules attached to surfaces have shown great potential as protein repellent moieties due to their flexibility and high level of hydration[17-20]. PEO chain length, as well as conformation and density of the polymer on the surface, are important parameters which determine resistance to protein adsorption[21,22]. Very low protein adsorption might indeed be achieved on surfaces which form a large number of hydrogen bonds with water molecules, leading to large repulsive forces towards proteins[23].

Mixed binary polymer brushes may be elaborated through the grafting of two polymers with different nature[24]. Each of the incorporated polymers might individually respond to an external stimulus, thus, a surface coating with a smart response to the environment can be prepared[25-30]. The combination of two or more polymers into the brush not only serves as an addition of different functions, but also affects the morphology of the brush. Uhlmann et al.[31] studied the adsorption of α-lactalbumin and α-chymotrypsin on polymer brushes composed of two polyelectrolytes: poly(2-vinyl-pyridine) (P2VP), a weak polybase, and PAA, a weak polyacid. By changing the pH and ionic strength of the solution, they regulated the amount of adsorbed proteins and the adsorption mechanism.

Mixed polymer brushes composed of a protein-adsorbing and a protein-repellent polymer are of particular interest owing to their ability to control protein adsorption. Hoy et al.[27] designed mixed brushes composed of PEG and of an amphiphilic block copolymer, poly(acrylic acid-*b*-styrene) (PAA-PS). The brush properties were controlled by the amount of PEG grafted on the surface and by applying external triggers such as ionic strength, pH, and Ca^{2+} concentration. As a control, fibrinogen adsorption was investigated on homobrushes: PS, PAA, PEG, and PAA-PS block

copolymer brushes. Protein adsorption was observed for all brushes; however, the lowest adsorption was observed on the PEG and PEG/PAA-PS mixed polymer brushes.

Delcroix et al.[32] studied human serum albumin (HSA) adsorption on pure PEO, PAA, and mixed PEO/PAA brushes. It was shown that the pure PEO brushes inhibited protein adsorption, as expected, while HSA adsorption was observed on pure PAA and mixed PEO/PAA brushes. The amount of adsorbed HSA was higher than the amount expected for a HSA monolayer formed on a solid substrate, showing the high adsorbing ability of PAA. It was also shown that 86% of HSA adsorbed on the PEO/PAA brushes was successfully desorbed at pH 9.0, and I=10^{-1}M, in conditions leading to the collapse of PAA, revealing the protein-repellent properties of PEO. An in-depth study of HSA adsorption on the pure PEO, PAA, and the mixed PEO/PAA brushes as a function of pH (from 3.0 to 9.0) and I (from 10^{-5}M to 10^{-1}M) was also performed[33]. The maximum adsorption of HSA was measured at I =10^{-5}M and pH 5.0. The amount of adsorbed HSA decreased with increasing ionic strength, and protein adsorption was observed even in conditions of electrostatic repulsion between PAA chains and HSA (pH 7.0). However, at pH 9.0, HSA adsorption on the PEO/PAA brushes was close to zero.

Adsorption and desorption studies of lysozyme (Lys), collagen (Col), and immunoglobulin G (IgG) were also conducted on the mixed PEO/PAA brushes[34]. It was demonstrated that the highest amount of Lys adsorbed on the PEO/PAA brushes was observed at pH 7.0 and low ionic strength (I = 10^{-5}M). It was also concluded that the best conditions for Lys desorption are at pH 3.5 and ionic strength 10^{-1}M. The highest amount of Col adsorbed on the PEO/PAA brushes was observed at high ionic strength and high pH values, while its desorption was observed at pH 3.0 and I = 10^{-3}M. IgG adsorption was performed at pH 7.4 and I = 10^{-5}M, and its desorption was conducted at pH 7.0 and I = 1.5x10^{-1}M. In this study, the effectiveness of mixed PEO/PAA brushes to reversibly adsorb and desorb HSA, Lys, Col, and IgG was demonstrated. The exact mechanism leading to the observed behavior was however not unraveled, and PEO chains were suspected to act both as spacing agents, leaving the PAA chains free to operate, and as protein-repellent moieties. Therefore, investigating the role of the PEO content of the brushes was identified as a way to better exploit the created mixed brushes.

With the present work, we aim to investigate the ability of smart mixed PEO/PAA brushes to adsorb and desorb proteins depending on brush composition and on environmental conditions, taking into account the number of PEO units per surface area and the ionic strength.

Mixed PEO/PAA polymer brushes were formed on a gold surface according to the "grafting to" method[35]. The properties of the brushes were tuned by modifying the PEO/PAA ratio, and the PEO chain length. The polymer brushes were formed by simultaneously grafting of thiol-terminated PEO and PAA to the gold surface, with varying PEO/PAA ratio in solution, to end up with a range of different PEO mass fractions in the mixed brushes[32]. Three proteins: HSA, Lys, and fibrinogen (Fb), very different from each other in size, shape and isoelectric point (iep), were chosen for the present study. HSA is the most abundant protein in blood and plays a very important role in biocompatibility. It is a globular protein with a molecular mass of 66 kDa and an iep close to 5.0[36-38]. To study electrostatic-dependent protein adsorption, lysozyme, with its iep at 11 and molecular mass of 14.3 kDa, was also chosen[39-41]. Additionally, HSA is considered as a soft protein, which can change its conformation after adsorption, while lysozyme is a hard protein and does not undergo conformational changes. The third chosen protein was Fb, a very large protein (340 kDa) with an iep situated at 5.8[42]. This protein, also very important for hemocompatibility issues, was chosen due to its reported[43-45] ability to adsorb above its iep. In the literature, it was reported that Fb adsorption on PAA brushes strongly depends on pH and ionic strength[46]. Below the iep of Fb, the adsorbed amount of the protein was found to increase with increasing pH, with a maximum at pH 5.8. Adsorption of Fb was also observed above its iep, where the protein and the brush interface are both negatively charged, and electrostatic repulsion is dominating. It was also shown that partial desorption of Fb from PAA brushes was achieved by rinsing the polymer brushes with salt solutions of different ionic strength (10^{-2} - 10^{-1} M) [46]. Taking into account all the reported data related to HSA, Lys and Fb adsorption on PAA brushes, protein adsorption studies on the mixed PEO/PAA brushes were carried out at pH 9.0 and at an ionic strength of 10^{-3} and 10^{-2}M. Protein desorption was performed at pH 9.0 and ionic strength equal to 0.15M.

EXPERIMENTAL SECTION

Materials

Gold substrates were prepared by thermal evaporation of gold (thickness of 100 nm) onto silicon wafers with the presence of a titanium interlayer. The gold-coated wafers were cleaved into pieces approximately 1 cm^2 in size for XPS measurements, and in the form of a rectangle having dimensions as described below for streaming potential measurements. Before every measurement, the gold substrates, as well as QCM quartz sensors (surface area of 1 cm^2) coated with a 100 nm Au layer, were cleaned in a mixture of 95% sulfuric acid (H_2SO_4, VWR BDH Prolabo, Leuven, Belgium) and hydrogen peroxide (30%, VWR BDH Prolabo, Leuven, Belgium) in a volume ratio of 2:1 for 2 min. Afterwards, the gold substrate was rinsed 10 times with deionized water, flushed with absolute ethanol, dried out in a stream of nitrogen gas and cleaned in a UV/ozone environment (Jelight INC., Irvine, USA) for 15 min. Next, it was rinsed again with absolute ethanol and dried under a gaseous nitrogen flow.

Thiol-terminated polymers were purchased from Polymer Source Inc. (Dorval, Canada). Poly(acrylic acid) (PAA) had a molar mass of M_n = 2000 g/mol, 23 repeating units, and a polydispersity index of 1.03. Poly(ethylene glycol) methyl ether was used with three molar masses: M_n = 1100 g/mol (~23 units-PEO1), M_n = 2000 g/mol (~43 units-PEO2), M_n = 5000 g/mol (~112 units-PEO5), and polydispersity indices of 1.08, 1.09, and 1.08, respectively. Stock solutions of polymers were prepared at a concentration of 5 g/L in ultrapure water and were further diluted in water to the desired concentration of 1g/L prior to each experiment. Synthesis of polymer brushes was conducted by the immersion of cleaned gold substrates in mixtures of PEO and PAA solutions, with PEO/PAA mass ratios of 100/0 (PEO), 10/90 (PEO/PAA 10/90), 50/50 (PEO/PAA 50/50), and 0/100 (PAA). The grafting method is illustrated in Scheme 1.

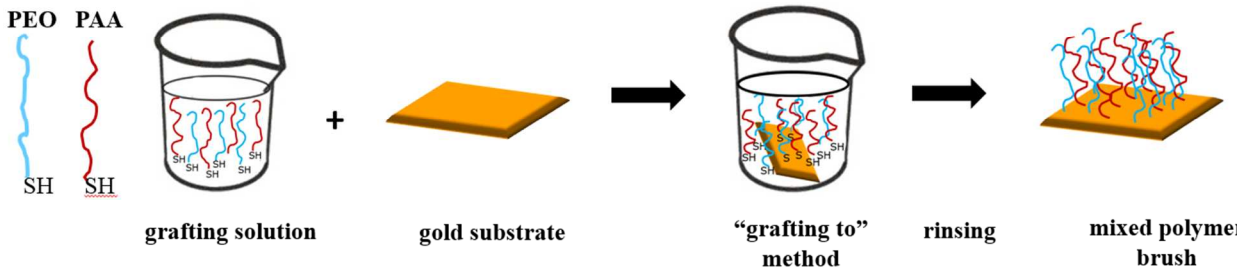

Scheme 1. Illustration of the method used for simultaneous grafting of PEO and PAA on a gold substrate (adsorption time = 60 min).

Human serum albumin (HSA, cat. no A 1653), lysozyme (Lys, cat no L 6876) and human fibrinogen (Fb, cat. no F3879) were purchased from Sigma-Aldrich. Protein stock solutions (1.0-3.0 mg/ml) were prepared under gentle stirring at pH 7.4, adjusted with NaOH, and $I = 10^{-3}$M, adjusted with NaCl, at room temperature. Next, the solution was passed through a 0.45 μm filter to eliminate aggregates and impurities and the concentration of the stock solution was spectrophotometrically (UV -1700 Spectrophotometer Shimadzu Inc., Japan) determined using the Bradford method[47]. Protein solutions of concentration equal to 0.2 mg/ml used for each experiment were prepared by diluting the stock solution in the sodium chloride solution of an appropriate *I*. The pH of each protein solution was adjusted to pH 9.0 by the addition of NaOH, and the ionic strength was regulated as indicated by the addition of NaCl.

A Purelab Ultra Elga instrument was used to purify water used in the experiments. Other chemical reagents such as sodium chloride and sodium hydroxide were purchased from Sigma-Aldrich and used without further purification.

Methods

X-ray Photoelectron Spectroscopy (XPS)

XPS measurements of the bare gold and gold samples with the polymer brushes were performed using a Kratos Axis Ultra spectrometer (Kratos Analytical, Manchester, UK) equipped with a monochromatized Al X-ray source. The pressure in the analysis chamber was 10^{-6} Pa and the direction of the photoelectrons during experiments was perpendicular to the sample. The analyzed area was 700×300 μm^2 and three measurements were performed for each sample on different sample spots. The pass energy used was 160 keV for the survey, and 40 eV for narrow scans. Charge stabilization was obtained by the Kratos axis device. XPS measurements for every sample consisted of the following steps: a) recording the survey spectra, b) recording C 1s, O 1s, S 2p, Au 4f spectra, and c) recording the C 1s spectra again to check the charge stability and absence of sample degradation. Data treatment was performed by the Casa XPS program (Casa Software Ltd., UK). Molar fractions (%) of every component were calculated using area of peaks after linear background subtraction.

Quartz Crystal Microbalance with Dissipation Monitoring (QCM-D)

Polymer brush formation and protein adsorption were monitored *in situ* by Quartz Crystal Microbalance (Q-Sense E4 System – Gothenborg, Sweden) at a temperature of 20^{o}C. The quartz crystal sensors coated with a 100 nm gold film were purchased from Q-Sense (Gothenborg,

Sweden). The measurements were started by obtaining a stable baseline for ultrapure water. Next, the polymer solution for grafting (PEO, PAA, PEO/PAA 10/90, or PEO/PAA 50/50) was flowed into the measurement cell with a flow rate of 20 μL/min. When a stable frequency and dissipation signals were obtained, ultrapure water was flushed again (flow rate = 50 μL/min) in order to remove loosely bound polymer molecules. Before every protein adsorption step, a saline solution of a desired I and pH (flow rate = 50 μL/min) was introduced in order to test the stimuli-responsive behavior of polymer brushes. The protein solution with a concentration of 0.2 mg/mL (at the same pH and I as in the previous step) was then flowed at the flow rate of 20 μL/min. Protein adsorption was continued until stable signals of frequency and dissipation were obtained. The rinsing/desorption procedure was performed at the flow rate of 50 μL/min, and it consisted of four stages: rinsing with the saline solution of the same pH and I as used for protein adsorption (R1), rinsing with ultrapure water (R2), introduction of a saline solution of 0.15M NaCl and pH 9.0 (R3), rinsing with ultrapure water (R4) (see Fig. 3).

The mass of deposited polymer(s) and adsorbed proteins per unit area was calculated from the Sauerbrey's equation[48]

$$\Delta m = -C\frac{\Delta f}{n} \quad (1)$$

where Δm is the change in mass, Δf is the measured frequency change, n is the overtone number and C is the sensitivity factor of the quartz sensor. Note that the Sauerbrey modeling is only applicable to uniform, rigid, thin films deposited on the sensor (i.e. when the $/\Delta D/\Delta f/$ ratio is lower than $0.4\text{x}10^{-6}$ Hz^{-1})[48]. This assumption was considered valid for all experiments (see Supporting Information Fig S-5.1). Frequency shifts were always measured between two baselines acquired in the same solution, as depicted in Figure 3.

Streaming Potential Measurements

Polymer brush formation and protein adsorption were also studied via streaming potential measurements using a homemade cell described in detail elsewhere[49,50]. The experimental conditions were the same as for the quartz crystal microbalance measurements. The main part of the cell was a parallel plate channel with dimensions of $2b_c \times 2c_c \times L = 0.027 \times 0.3 \times 3.5$ cm^3 formed by gold substrates separated by a perfluoroethylene spacer. The streaming potential E_s was measured as a function of the hydrostatic pressure ΔP of driving electrolyte flows through the channel, using a pair of Ag/AgCl electrodes. The overall cell electric conductivity, K_e, was

determined using a pair of Pt electrodes. Knowing the slope of the ΔE_s vs. ΔP dependence, the apparent zeta potential (ζ) of each substrate surface was calculated from the Smoluchowski relationship:

$$\zeta = \frac{\eta L}{4\varepsilon b_c c_c R_e}\left(\frac{\Delta E_s}{\Delta P}\right) = \frac{\eta K_e}{\varepsilon}\left(\frac{\Delta E_s}{\Delta P}\right) \quad (2)$$

where η is the dynamic viscosity of the solution, ε is the dielectric permittivity, and R_e is the net electric resistance of the cell, which is the sum of the bulk and surface resistances. The measurements were performed at $I = 10^{-2}$M, pH 9.0 on pure homobrushes, mixed PEO/PAA brushes, and brushes after protein adsorption.

Atomic Force Microscopy

Atomic Force Microscopy analyses were performed using a Nanoscope III instrument (Digital Instruments, Santa Barbara, USA) in tapping mode. The probes, made of Si, had a spring constant between 10 and 130 N/m and resonance frequency 204-497 kHz (Nanosensors, Switzerland). The scan rate was 1 Hz. Images were plane-fitted and flattened using the image analysis software provided with the microscope. The image size was 2 x 1 μm^2.

RESULTS AND DISCUSSION

This section is divided into three parts. In the first part, polymer brush characterization is presented as a function of PEO/PAA ratio and PEO molar mass. The second part presents studies related to protein adsorption/desorption on the pure PEO and PAA brushes. The third part is devoted to protein adsorption/desorption on the mixed PEO/PAA polymer brushes as a function of PEO molar mass.

Polymer Brush Characterization – Effect of PEO/PAA Ratio and PEO Molar Mass

Surface molar fractions of all elements recorded by XPS for the homo and the mixed PEO/PAA brushes are presented and discussed in detail in Table S-1.1 in the Supporting Information (SI).

Figure 1 illustrates C 1s peaks recorded by XPS on a gold surface modified with thiol-functionalized polymers. The C 1s peak decomposition of PEO and PAA (see Fig.1a and Fig.1b) was performed according to the method described in SI-S1. It can be noticed that, in Fig.1a, the **C**-O-**C** component at 286.3 eV attributed to PEO is dominating the spectrum. However, there is

also a small **C**-OOH component at 288.8 eV attributed to contaminants. In Fig. 1b, the much larger **C**-OOH component is mainly attributed to the COOH group of PAA. The respective presence of the **C**-O-**C** and C-OOH components proves that PEO and PAA were successfully attached to the gold substrate.

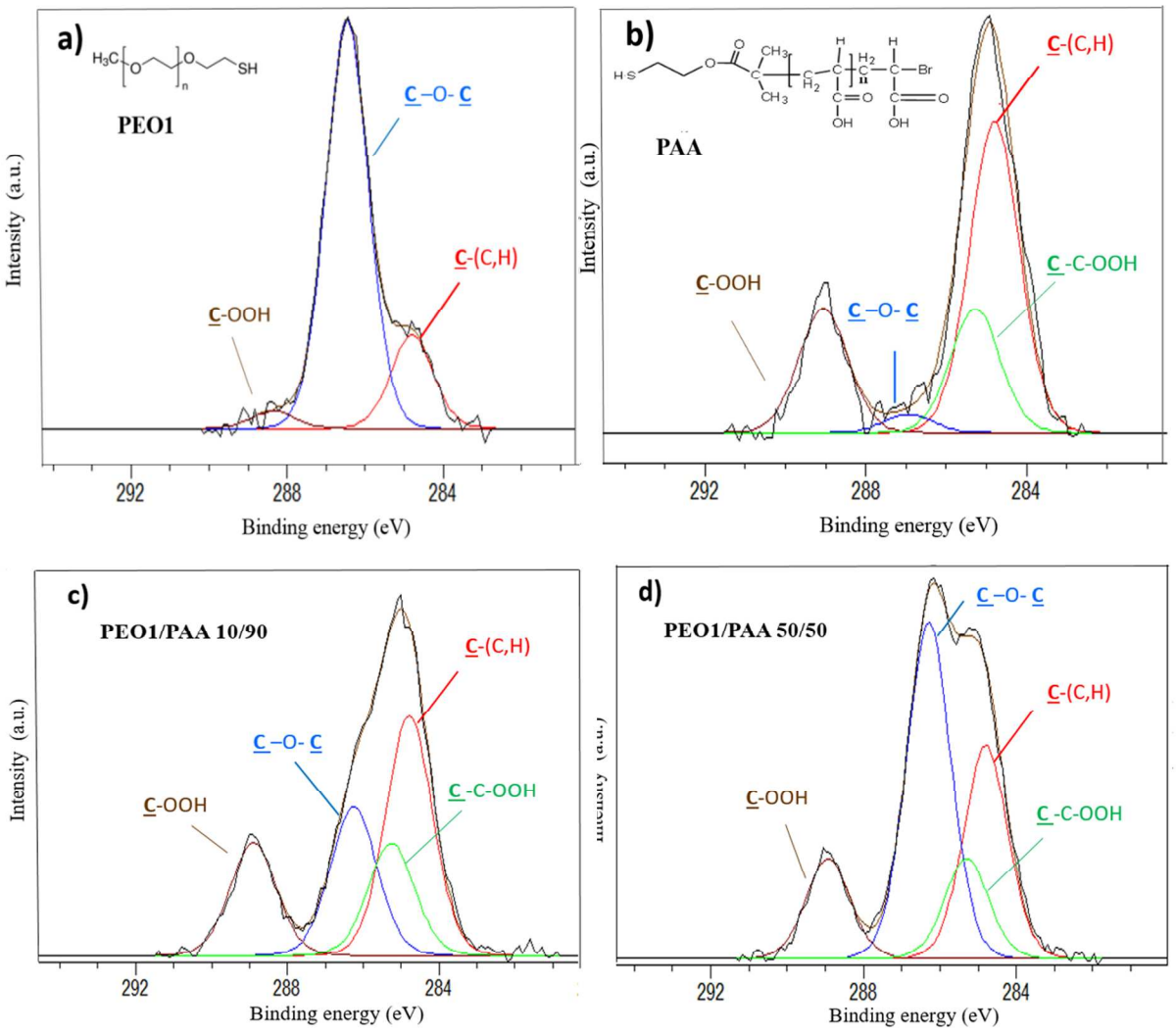

Figure 1. C 1s peaks recorded by XPS on gold surfaces modified with thiol-functionalized polymers: a) PEO1, b) PAA, c) PEO1/PAA 10/90, d) PEO1/PAA 50/50. Peak decomposition was performed according to the protocol described in SI-S1.

Figures 1c and 1d present C 1s peaks recorded for the PEO1/PAA 10/90 and PEO1/PAA 50/50 mixed brushes. It can be observed that, in both cases, the **C**-O-**C** component at 286.3 eV

attributed to PEO, as well as the **C**-OOH component at 288.8eV attributed to PAA, are present in the recorded spectra, and their proportions depend on the PEO/PAA ratio: a larger **C**-O-**C** peak component and a smaller **C**-OOH component are observed when more PEO was introduced in the grafting solution (see Fig.1d vs Fig.1c).

Figure 2 presents the dependence of **C**-OOH, **C**-O-**C** and Au surface atomic fraction (%) on the molar mass of PEO for PEO/PAA 10/90 (Fig.2a) and 50/50 (Fig.2b) brushes. For PEO/PAA 10/90 mixed brushes, a slight decrease of the carbon attributed to the **C**OOH group of PAA is observed with increasing PEO molar mass (from 10 to 9.2% for PEO1/PAA 10/90 and PEO5/PAA 10/90, respectively), while the **C**-O-**C** fraction increases significantly (from 13.7 to 23.5% for PEO1/PAA 10/90 and PEO5/PAA 10/90, respectively). On the other hand, the atomic fraction of gold decreases with higher molar mass of PEO (from 26.6% for PEO1/PAA 10/90 to 18.3% PEO5/PAA 10/90). It proves that longer PEO chains, together with PAA, efficiently cover the gold surface. Mixed PEO/PAA 50/50 brushes show the same tendencies as the PEO/PAA 10/90 brushes. The **C**-OOH atomic fraction slightly decreases from 6.9 to 5.8 % for PEO1/PAA 50/50 and PEO5/PAA 50/50, respectively. These values are lower in comparison to PEO/PAA 10/90 brushes and indicate lower amounts of PAA in the brushes as expected from the composition of the solutions used for grafting. Conversely, the **C**-O-**C** fraction attributed to PEO is higher than for PEO/PAA 10/90 brushes. It should be highlighted that the surface atomic fraction of Au and of **S**-Au (Table S-1) is higher for PEO/PAA 50/50 brushes in comparison to the PEO/PAA 10/90 brushes.

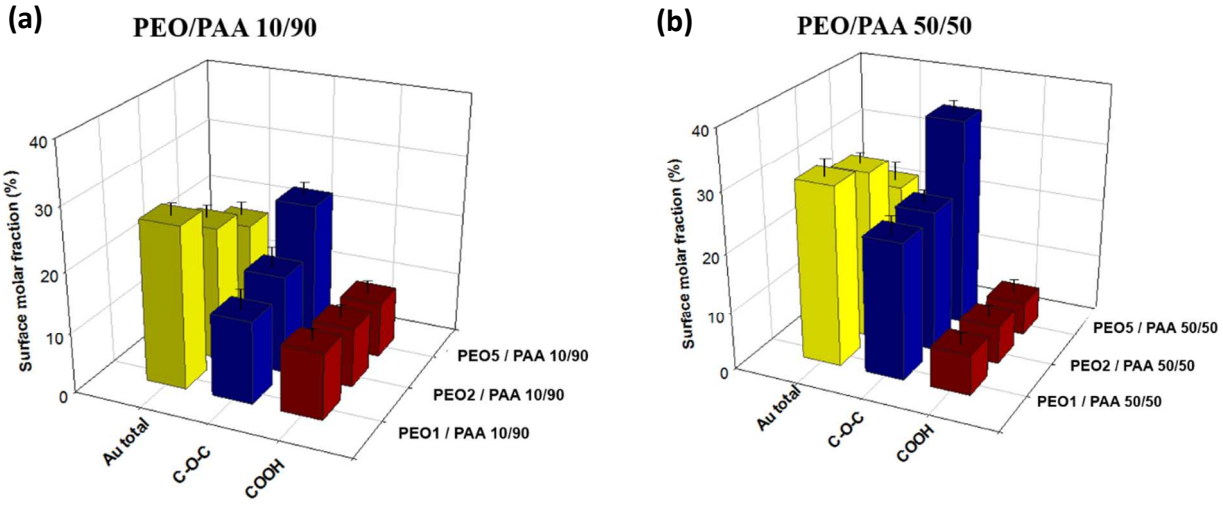

Figure 2. Dependence of **C**-OOH, **C**-O-**C** and Au surface atomic fraction (%) recorded by XPS on the molar mass of PEO: a) PEO/PAA 10/90, b) PEO/PAA 50/50.

Table 1. Characterization of homo and mixed polymer brushes formed on gold: *d** - average thickness of dry polymer brushes extracted from XPS measurements, PEO units – number of PEO units per nm^2, PAA units – number of PAA units per nm^2, Δm - wet mass per unit area obtained from the Sauerbrey modeling of Δf measured by QCM-D, *d*** - average thickness of wet polymer brushes extracted from QCM-D data taking into account density of PEO (1.13 g/cm^3) and PAA (1.074 g/cm^3), ζ - zeta potential measured at $I = 10^{-2}$M, pH 9.0.

Sample name	*d** (nm)	PEO units (nm^2)	PAA units (nm^2)	Δm (ng/cm^2)	*d*** (nm)	ζ (mV)
Au	-	-	-	-	-	-56 ± 6
Au-PAA	2.6 ± 0.2	-	35	475.0 ± 76	4.4	-39 ± 5
Au-PEO1	1.6 ± 0.3	12	-	547.0 ± -56	4.8	-35 ± 4
Au-PEO2	1.9 ± 0.3	28	-	675.0 ± 63	6.0	-36 ± 4
Au-PEO5	2.9 ± 0.2	45	-	1195.0 ± 50	10.2	-32 ± 4
Au-PEO1/PAA 10/90	3.5 ± 0.3	16	17	497.0 ± 84	4.5	-43 ± 5
Au-PEO2/PAA 10/90	4.1 ± 0.3	22	20	580.0 ± 65	5.3	-41 ± 5
Au-PEO5/PAA 10/90	4.7 ± 0.2	22	23	1275.0 ± 45	11.6	-40 ± 5
Au-PEO1/PAA 50/50	3.0 ± 0.3	25	9	520.0 ± 78	4.7	-40 ± 4
Au-PEO2/PAA 50/50	3.2 ± 0.3	27	9	560.0 ± 60	5.1	-42 ± 4
Au-PEO5/PAA 50/50	3.9 ± 0.3	34	14	1196.0 ± 55	10.9	-35 ± 4

The thickness *d** of polymer brushes was calculated from XPS data (see Table 1, details in S-2 section). The pure PAA layer has a thickness of 2.6 nm, while the pure PEO layers have a thickness which increases with the molar mass of PEO, from 1.6 to 2.9 nm for PEO1 and PEO5, respectively. The thickness of the mixed polymer brushes is higher than the one of pure PEO and PAA brushes, which is attributed to the higher density of these mixed brushes. This is in agreement with the better coverage of the gold substrate by mixed brushes (see Table S-1). Moreover, higher values of thickness are observed in the case of PEO/PAA 10/90, compared to PEO/PAA 50/50 brushes, and thickness is also increasing with increasing molar mass of PEO.

Furthermore, taking into account the thickness (*d**) of the dry PEO and PAA homobrushes, and the density of both polymers (PEO: 1.13 g/cm^3, PAA: 1.074 g/cm^3 [51]), the dry grafted polymer

mass and the number of corresponding PEO and PAA units per nm^2 were calculated (see Table 1). The number of PEO and PAA units per nm^2 in the mixed brushes was also estimated, based on the volumetric fraction of each polymer obtained from XPS data, according to a method described previously [32]. The number of PEO units per nm^2 in the pure PEO brushes increases from 12 to 45 for PEO1 and PEO5, respectively, while for pure PAA, the number of PAA units per nm^2 is equal to 35. For the mixed PEO/PAA 10/90 brushes, the number of PEO units per nm^2 increases with increasing PEO molar mass, from 16 for PEO1/PAA 10/90 to 22 for PEO5/PAA 10/90 brushes. The number of PAA units per nm^2, for the same brushes, increases from 17 to 23. In contrast to the PEO/PAA 10/90 brushes, the brushes created with the ratio of PEO/PAA 50/50 contain less PAA (from 9 to 14 units per nm^2 for PEO1/PAA 50/50 and for PEO5/PAA 50/50, respectively), while the number of PEO units per nm^2 also increases with the PEO molar mass (from 25 for PEO1/PAA 50/50 to 34 for PEO5/PAA 50/50 brushes). The influence of the number of PEO and PAA units per unit of surface area on adsorption and desorption of proteins is discussed later. The number of PEO and PAA chains per nm^2 was also used to demonstrate that homobrushes are in the intermediate (PEO1, PEO2) or in the brush regime (PEO5, PAA), while all mixed brushes are in the brush regime (see S-3 section).

The layer thickness of polymer brushes was also estimated from QCM measurement (see Table 1, d^{**}). Typical QCM experiments including polymer brush formation are presented in Fig. 3. After stabilization under water, the polymer solution (PEO1/PAA 10/90 or PEO1/PAA 50/50) was flowed into the cell, allowing a frequency shift corresponding to the polymer brush formation to be measured. The frequency shift Δf_1 stabilizes and does not change significantly during rinsing with pure water. The corresponding wet mass per unit area (Δm) of polymer brushes was calculated and is presented in Table 1. Next, by taking into account the density of both polymers, d^{**} values were calculated. Note that, since the density of the polymers is not very far from the one of water, the error made when transforming the mass into thickness is of less than 10%. The d^{**} extracted from QCM-D are equal to 4.4 nm and 4.8 nm for PAA and PEO1, respectively. The thickness values extracted from QCM-D measurements are not in agreement with the XPS data: d^{**} of PAA is lower than d^{**} of PEO1 while the reverse situation is found for d^{*}. Mixed brushes formed with the PEO/PAA ratio of 10/90 and 50/50 present similar d^{**} thicknesses for a given PEO molar mass. Brushes containing PEO5 are significantly thicker than all other brushes. It has to be highlighted that Δm are measured by QCM as a wet mass per unit area, while thickness d^{*}

is extracted from XPS data obtained on dry samples. Therefore, the observed differences between QCM-D and XPS data are assigned to the differences in layer water content. Because d^{**} of PEO1 is higher than d^{**} of PAA, while d^{*} shows the reverse trend, it can be concluded that the PEO layer is more hydrated than the PAA layer. From the comparison of thickness values for dry and wet layers (d^{*} vs d^{**}), the water content of polymer layers is in the range of 25 to 75%. Mixed brushes containing PEO5 are much more hydrated than the ones containing PEO1 and PEO2.

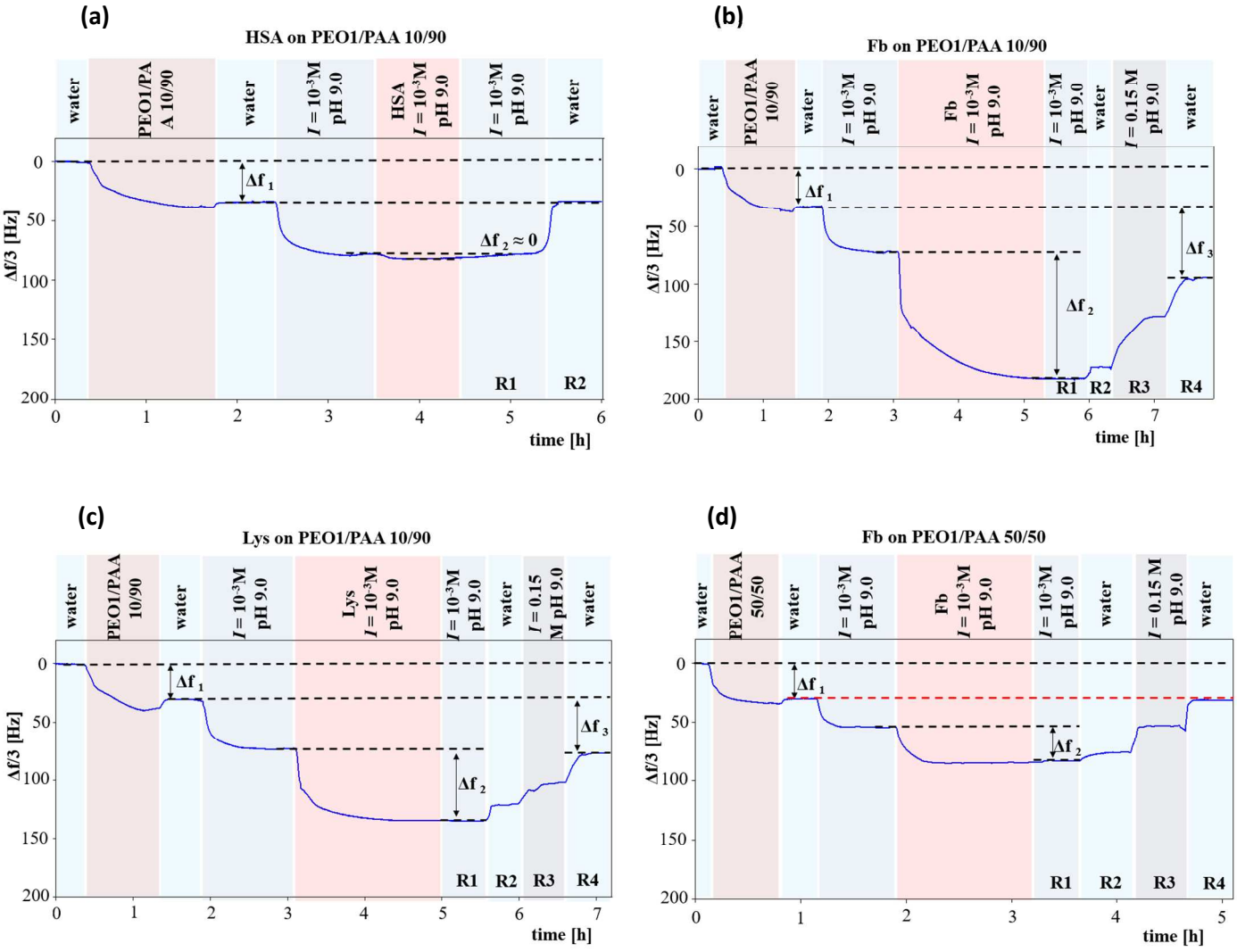

Figure 3. QCM graphs of PEO/PAA mixed brushes formation on a gold surface, followed by steps of adsorption (I = 10^{-3}M, pH 9.0) and desorption (I =0.15M, pH 9.0) of proteins (c = 0.2 mg/ml): a) HSA on PEO1/PAA 10/90 brushes, b) Fb on PEO1/PAA 10/90 brushes, c) Lys on PEO1/PAA 10/90 brushes, d) Fb on PEO1/PAA 50/50 brushes. R1- Rinsing with a saline solution of the same pH and ionic strength as used for protein adsorption, R2 - rinsing with

ultrapure water, R3 - introduction of a saline solution of 0.15M and pH 9.0, R4 - rinsing with ultrapure water.

In order to determine the electrokinetic properties of the homo and mixed PEO/PAA brushes, streaming potential measurements were performed. First, measurements were done on a bare gold surface, and the corresponding zeta potential was equal to -56 mV (see Table 1). Similar values of zeta potential in neutral solutions were previously reported in the literature.[52] Next, electrokinetic measurements were conducted for pure PEO and PAA brushes. The zeta potential of the grafted PEO and PAA brushes was significantly less negative than the one of bare gold: -39 mV for pure PAA, and in the range of -32 to -36 mV for PEO brushes. The zeta potentials for mixed polymer brushes laid between -43 and -35 mV and cannot be used to distinguish them from each other. Additionally, to check the homogeneity of the distribution of polymers in homo- and mixed brushes, images were performed by Atomic Force Microscopy (Figure S-4.1). At the probed scale, no aggregates could be observed.

The results show that, in all cases, both polymers are well present in the mixed PEO/PAA 10/90 and PEO/PAA 50/50 brushes. The results also reveal that the number of PEO repeating units increases with increasing molar mass of PEO for the PEO/PAA 10/90 and PEO/PAA 50/50 brushes, while the number of PEO and PAA units are respectively lower and higher for the PEO/PAA 10/90 brushes in comparison to the PEO/PAA 50/50 brushes. The thickness of the mixed PEO/PAA 10/90 and PEO/PAA 50/50 brushes increases with increasing PEO molar mass, which is attributed to the higher density of the mixed polymer brushes.

Protein Adsorption on Pure PEO and PAA Polymer Brushes

Protein-repellent properties of PEO brushes were studied using QCM and streaming potential measurements. As an illustration of the protein-repellent properties of PEO brushes, a QCM-D experiment of HSA adsorption on the PEO1 brush was selected and is presented in Fig. S-5.1. Similar experiments were performed with Lys and Fb for polymer brushes formed from PEO1, PEO2 and PEO5. Results showing the repellent properties of PEO1 towards HSA, Fb, and Lys adsorption are presented in Fig.4 (data on the far left of each graph). Streaming potential measurements, performed after adsorption of HSA, Fb, and Lys on PEO1 brushes show negligible changes in zeta potential that can be interpreted as a lack of protein adsorption, in line

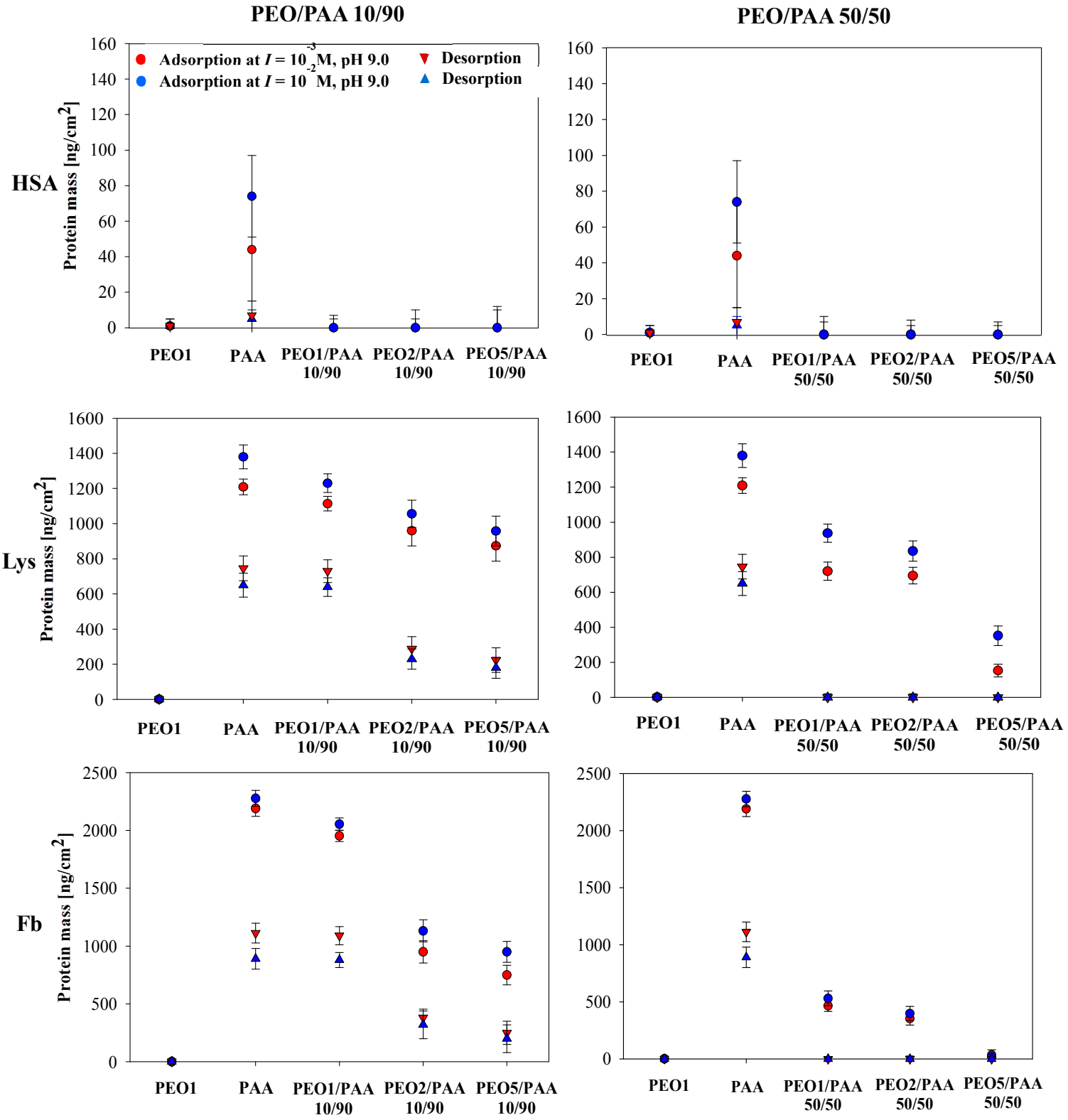

with QCM data (see Fig.5 data on the far left of each graph). Similar results were obtained for PEO2, and PEO5 brushes (not presented).

Figure 4. Protein mass obtained from the Sauerbrey modeling of Δf measured by QCM-D after adsorption on PEO1, PAA homobrushes, and the mixed PEO/PAA 10/90 (left) or PEO/PAA 50/50 (right) brushes. Top: HSA, middle: Lys, bottom: Fb. Red - adsorption at $I = 10^{-3}$M pH 9.0,

blue – adsorption at I=10^{-2}M pH 9.0, circles – adsorbed mass, triangles – residual mass after desorption at I =0.15M, pH 9.0.

Conversely, the pure PAA brushes adsorbed Lys and Fb (see Fig.4 middle, bottom), while the adsorption of HSA was negligible (less than 80 ng/cm^2, see Fig.4 top). The average adsorbed mass of HSA at I = 10^{-3}M, pH 9.0, was 44 ng/cm^2 while at I = 10^{-2}M, pH 9.0 it was 74 ng/cm^2. Partial desorption of HSA from the pure PAA brushes was observed, and the remaining HSA mass was close to 10 ng/cm^2 for adsorption performed at I = 10^{-3}M and I = 10^{-2}M. This experiment was also monitored by streaming potential measurements, and is presented in Fig. 5a. The zeta potential changes upon adsorption and desorption of HSA were not significant.

It should be noted that protein adsorption from a single protein solution on pure PAA brushes was also performed at I = 0.15M, pH 9.0. Under these conditions, negligible adsorption was observed for Lys and Fb. An example of such an experiment, illustrating Lys adsorption on the PAA brushes at I = 0.15M, pH 9.0 is presented in Fig. S-6.1. These conditions were accordingly chosen to trigger the protein desorption process.

Regarding Lys adsorption on the pure PAA brushes at I = 10^{-3}M and I = 10^{-2}M (Fig.4 middle), the calculated masses of the protein were equal to 1210 ng/cm^2 and 1380 ng/cm^2, respectively. Partial desorption of Lys was only observed (Lys mass close to 700 ng/cm^2). Streaming potential measurements showed a significant shift in zeta potential from -39 mV to -5 mV before and after Lys adsorption (see Fig.5 b). It is worth mentioning that the zeta potential of the PAA brush with adsorbed Lys does not reach the zeta potential value of Lys measured in bulk, i.e. + 8.5 mV for I = 10^{-2}M, pH 9.0[53]. This effect was previously observed and thoroughly described for polyelectrolyte[50,54], polypeptide[55], and protein[56] monolayers. Furthermore, desorption of Lys from the brushes results in a zeta potential of about -20 mV, indicating a partial desorption. Lys adsorption on the PAA brushes was also studied by Delcroix et al.[34] who observed 700 ng/cm^2 of Lys on pure PAA brushes (I = 10^{-2} M, pH 7.4), and a partial desorption was performed at I = 0.1M, pH 3.0.

For fibrinogen, the adsorbed masses on the pure PAA at I = 10^{-3}M and I = 10^{-2}M were equal to 2190 ng/cm^2 and 2277 ng/cm^2 (Fig.4 bottom). The measured Fb mass after desorption was close to 1000 ng/cm^2. Streaming potential measurements of PAA brushes after Fb adsorption also showed significant changes of zeta potential, indicating effective adsorption (see Fig.5c). The zeta potential of the PAA brush with the Fb layer reached -20 mV, which is close to the value of

the Fb zeta potential measured in the bulk (-18 mV, $I = 10^{-2}$M, pH 9.0[45]), and agrees with the literature data of the zeta potential for Fb adsorbed on positively-charged microspheres.[57] It is worth mentioning here that protein adsorption is observed on the "wrong" side of the isoelectric point, as previously reported in the literature.[58-60]. This is attributed to heterogeneous charge distribution over the Fb molecules (the presence of the side arms bearing the positive charge despite of the negative overall charge of the Fb molecule) allowing the adsorption of Fb molecules at basic pH.[58,61,62]

After desorption, the zeta potential changed to – 25 mV, which also indicates a partial desorption. Fibrinogen adsorption on PAA was also performed by Psarra[63] who measured about 4000 ng/cm^2 of Fb adsorbed on PAA (25 kDa) Guiselin brushes at pH 7.0 and $I = 10^{-2}$ M. In that study, the adsorption experiment was performed with 0.25 mg/mL of the protein and was monitored by *in situ* spectroscopic ellipsometry. Desorption experiments were performed at I = 0.05M but complete protein desorption was not observed.

Adsorption of HSA on the "wrong" side of its isoelectric point was also reported, but for pH values up to about 7.[33,64] At pH 8.5 already, the electrostatic repulsion becomes predominant and adsorption is strongly decreased.[64] Fb and HSA may behave differently at pH 9 in reason of the slightly higher isoelectric point of Fb, but also of their different amino acid sequence and conformation, that influence the distribution of positively charged patches.

For all proteins, the adsorbed mass was slightly higher at $I = 10^{-2}$M compared to 10^{-3}M. At this *I,* more counterions screen the charges of PAA and proteins. PAA chains are still swollen and the higher screening of protein charges allows the proteins to be more packed in the polymer brush. The conformational changes of PAA and their influence on the protein adsorption behavior were discussed in detail previously.[33]

From these results, it can be concluded that pure PEO brushes inhibit HSA, Lys, and Fb adsorption. We also showed negligible adsorption of HSA on the PAA brushes. Lys and Fb, on the other hand, adsorb on the pure PAA brushes but their total desorption was not achieved in the selected conditions.

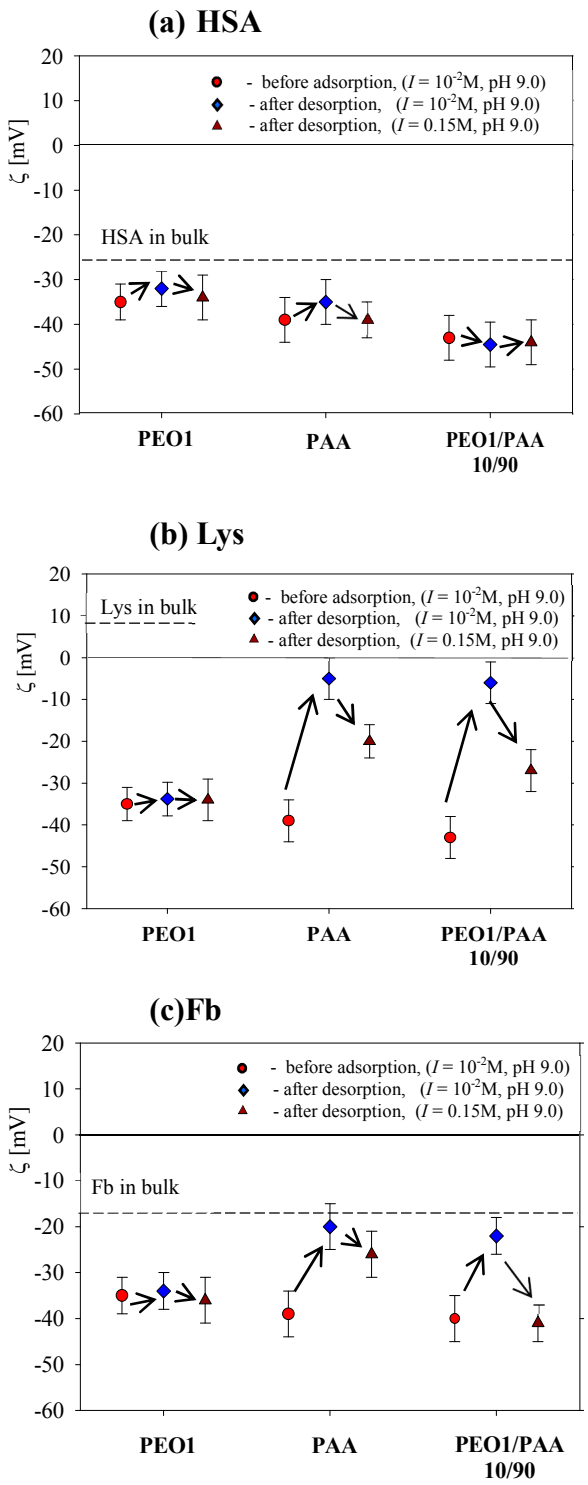

Figure 5. Zeta potential (ζ) of pure PEO1, PAA brushes, and PEO1/PAA mixed brushes before protein adsorption, $I = 10^{-2}$M, pH 9.0, (red closed symbols), after protein adsorption $I = 10^{-2}$M, pH 9.0, (blue diamonds), and after protein desorption, I = 0.15M, pH 9.0 (brown triangles); a) HSA adsorption/desorption on pure PEO1, PAA, and PEO1/PAA 10/90 brushes, b) Lys adsorption/desorption on pure PEO1, PAA, and PEO1/PAA 10/90, c) Fb adsorption/desorption on pure PEO1, PAA, and PEO1/PAA 50/50. The dashed line shows the value of zeta potential of proteins measured elsewhere [42,53,60].

Protein adsorption on mixed PEO/PAA 10/90 and PEO/PAA 50/50 polymer brushes

HSA, Lys, and Fb adsorption experiments were also performed on the mixed PEO/PAA 10/90 and PEO/PAA 50/50 brushes with PEO of different molar masses. In all cases, the frequency shift Δf_2 was used to calculate a protein mass after the adsorption step, while Δf_3 was used to estimate protein mass after the desorption step (see Fig.3). Streaming potential measurements of the mixed polymer brushes were performed only for PEO1/PAA 10/90 brushes (HSA, Lys adsorption/desorption), and PEO1/PAA 50/50 brushes (Fb adsorption/desorption) in order to support or confirm results obtained from QCM experiments.

Figure 3a shows a QCM graph of HSA adsorption on the PEO1/PAA 10/90 polymer brush.

It can be concluded that polymer brushes were successfully formed on the gold crystal and that there is no HSA adsorption at pH 9.0 and $I = 10^{-3}$M ($\Delta f_2 \sim 0$). Similar results were obtained for the mixed PEO2/PAA 10/90, PEO5/PAA 10/90 brushes and for the PEO/PAA 50/50 brushes (see Fig. 4 top). The mass of HSA after the adsorption step is close to zero for PEO/PAA 10/90 and PEO/PAA 50/50 brushes. In addition, streaming potential measurements for HSA adsorption/desorption on PEO1/PAA 10/90 brushes show negligible changes in the electrokinetic properties of the system (see Fig. 5a), which supports the statement of negligible HSA adsorption.

Fibrinogen adsorption on PEO1/PAA 10/90 polymer brushes is presented in Fig. 3b. The mass of Fb adsorbed on the PEO1/PAA brush, calculated from Δf_2, was equal to 1953 ng/cm^2. The next two shifts correspond to the rinsing with ultrapure water (R2) and the desorption step with a 0.15M, pH 9.0 saline solution (R3). Finally, the Δf_3 shift corresponds to the remaining mass of Fb after the last desorption step in ultrapure water (1114 ng/cm^2). Fig. 3 (middle, left) represents Lys adsorption and desorption on PEO1/PAA 10/90 brushes. In this case, the calculated mass of Lys after the adsorption step was 1178 ng/cm^2, and the remaining protein mass after the desorption step was equal to 795 ng/cm^2. This latter experiment was also studied by streaming potential as presented in Fig. 5b, which shows a significant shift in zeta potential from -43 mV to -6 mV before and after Lys adsorption. Similarly to the zeta potential changes after Lys adsorption on the pure PAA brushes, the zeta potential does not reach the zeta potential value of Lys measured in bulk. However, desorption of Lys from the PEO1/PAA 10/90 brushes results in a zeta potential of about -26 mV indicating a partial desorption, but more effective in comparison to the

desorption on the pure PAA brush (zeta potential of -20 mV). It proves that PEO plays an important role in the protein desorption process, as already demonstrated earlier in other conditions[34].

Fig. 3d shows a QCM graph of Fb adsorption on the PEO1/PAA 50/50 polymer brush. The calculated Fb mass after the adsorption step was 520 ng/cm^2. After the rinsing with water (R1-R4), a total desorption of Fb was observed. This experiment was also studied by streaming potential measurements as presented in Fig. 5c. The zeta potential changed from – 40 mV for the PEO1/PAA 50/50 brush to – 22 mV after Fb adsorption, while after desorption, it changed back to – 41 mV indicating total desorption. These observations on mixed PEO/PAA brushes confirm previous statements about the strong influence of PEO on the protein desorption process.

A summary of the results obtained for the adsorption of HSA, Fb and Lys at $I = 10^{-3}$M and $I = 10^{-2}$M, pH 9.0 on the pure PEO1, PAA brushes, and the mixed PEO/PAA brushes as a function of PEO molar mass is presented in Fig. 4. The highest amount of Lys was observed on the pure PAA brushes (1380 ng/cm^2, see previous section) at $I = 10^{-2}$M, pH 9.0, and it decreased while increasing the molar mass of PEO from 1230 ng/cm^2 to 958 ng/cm^2 for PEO1/PAA 10/90 and PEO5/PAA 10/90 brushes, respectively. A further decrease in the Lys masses adsorbed at $I = 10^{-2}$M, pH 9.0 was observed after adsorption on PEO/PAA 50/50 brushes. The calculated masses of Lys changed from 937 ng/cm^2 for PEO1/PAA 50/50 brushes to 352 ng/cm^2 for PEO5/PAA 50/50 brushes. Similar tendencies were observed after adsorption at $I = 10^{-3}$M on both mixed brushes (Fig. 4 middle).

Similarly to Lys, the highest amount of Fb was observed after adsorption on the pure PAA brushes at $I = 10^{-2}$M (2277 ng/cm^2), as discussed in detail in the previous section, and it decreased while increasing the molar mass of PEO, and its amount in the mixed PEO/PAA brushes. For example, the amount of Fb adsorbed on PEO1/PAA 10/90 brushes at $I = 10^{-2}$M, pH 9.0 was equal to 2054 ng/cm^2 while on PEO1/PAA 50/50 it was 530 ng/cm^2. A more significant decrease in the Fb mass was observed after adsorption on PEO5/PAA brushes at $I = 10^{-2}$M and it changed from 950 ng/cm^2 for PEO5/PAA 10/90 brushes to 20 ng/cm^2 for PEO5/PAA 50/50 brushes. Similar tendencies were observed for Fb adsorption at $I = 10^{-3}$M on PEO/PAA 10/90, and PEO/PAA 50/50 brushes (see Fig. 4 bottom).

The results derived from the desorption experiments of Lys and Fb from the pure PAA and the mixed PEO/PAA brushes monitored by QCM-D at $I = 0.15$M, pH 9.0 are presented in Fig 4

(triangles). The highest amount of Lys after desorption was measured on the pure PAA brush (746 ng/cm^2) and it decreased, while increasing the molar mass of PEO (from 730 ng/cm^2 to 224 ng/cm^2 for PEO1/PAA 10/90 and PEO5/PAA 10/90, respectively). On PEO/PAA 50/50 brushes, Lys desorption was totally achieved whatever the molar mass of PEO (see Fig. 4 middle - triangles).

The same trends were observed for Fb. A partial desorption of Fb was observed on the PAA and the PEO/PAA 10/90 brushes. The highest amount of Fb after desorption was observed for the pure PAA brushes (1113 ng/cm^2 – adsorption at I =10^{-3}M). The remaining amounts of Fb on the brushes after desorption decreased while increasing the molar mass of PEO. For example, for the PEO1/PAA 10/90 brush, it was 1090 ng/cm^2 (adsorption at I =10^{-3}M), while for the PEO5/PAA 10/90 brush, it was 250 ng/cm^2 (adsorption at I =10^{-3}M). Desorption was totally achieved on all PEO/PAA 50/50 brushes.

Fig.6 presents the dependence of protein mass (Fig. 6 a,b for Lys and Fb, respectively) obtained from the Sauerbrey modeling of Δf measured by QCM-D after the adsorption step (R1, I = 10^{-2}M, pH 9.0), and the desorption step (R4, I = 0.15M, pH 9.0), as a function of the number of PEO units per nm^2 obtained from XPS measurements (Table 1). Both the protein adsorbed amount and the remaining amount after desorption decrease with increasing number of PEO units per unit of surface area in the brush. PEO chains play the role of protein-repellent moieties, and their increasing presence leads to decreased PAA density as well. For this reason, the brushes which contain higher amounts of PEO units, regulated either by the PEO/PAA ratio in solution used for grafting or by PEO molar mass, adsorb lower amounts of protein. These brushes are also most suitable if total desorption of proteins is expected.

In order to both effectively adsorb and desorb Lys, ie to obtain a fully reversible behavior, 25 to 34 units of PEO must be present in the mixed PEO/PAA brush. For effective adsorption/desorption of Fb from the mixed PEO/PAA brushes, the operational window is restricted to 25 to 27 units of PEO in the mixed PEO/PAA brush.

In this section, we showed that HSA does not adsorb on the mixed PEO/PAA 10/90 and PEO/PAA 50/50 brushes. Lys and Fb on the other hand adsorb on the PEO/PAA 10/90 and PEO/PAA 50/50 brushes, and the amount of adsorbed protein decreases while increasing the molar mass of PEO, or its amount in the polymer brush. The mass of adsorbed proteins depends slightly on the ionic strength, with higher values measured at I =10^{-2}M compared to 10^{-3}M. A

partial desorption of Lys and Fb was observed on the mixed PEO/PAA 10/90 brushes, while total desorption was observed for the PEO/PAA 50/50 brushes. A minimum of 25 PEO units per nm^2 is required to achieve total desorption.

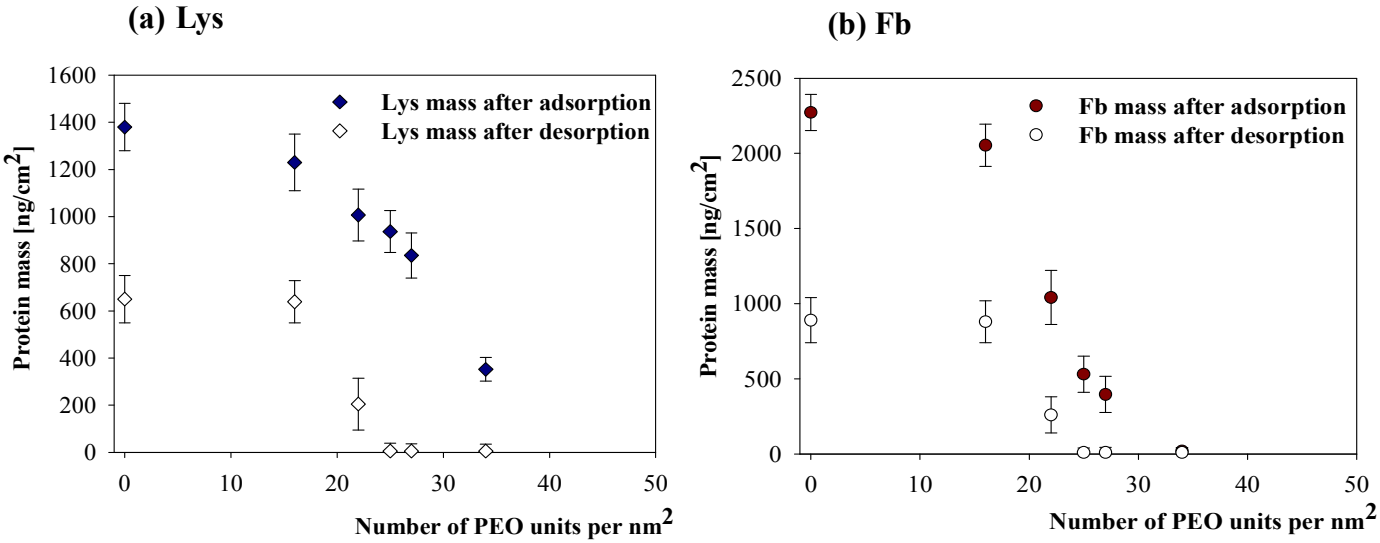

Figure 6. Dependence of protein mass obtained from the Sauerbrey modeling of Δf measured by QCM-D after adsorption step (closed symbols - R1, $I = 10^{-2}$M, pH 9.0), and desorption step (open symbols - R4, I = 0.15M, pH 9.0), as a function of PEO units per nm^2 obtained from XPS measurements: a) Lys, b) Fb.

CONCLUSIONS

With this work, we demonstrate the effectiveness of mixed PEO/PAA brushes to reversibly adsorb human fibrinogen and lysozyme. The role of the amount of PEO in the brushes, regulated by changing its molar mass or its fraction in the solution used for polymer grafting, is elucidated. HSA adsorption is negligible on the pure PAA and on the mixed PEO/PAA brushes. The amount of adsorbed Lys and Fb decreases while increasing the PEO content of the mixed brushes. Under the selected I and pH conditions, protein adsorption is mainly governed by the swelling/collapse behavior of PAA chains and by the contribution of electrostatic interactions. The adsorbed proteins can be completely removed only from the PEO/PAA mixed brushes with a minimum of 25 PEO units per nm^2. The desorption is believed to be triggered by the exposure of PEO chains upon PAA shrinking. Since the three proteins are different in size, shape and iep, the reversible behavior of the mixed PEO/PAA brushes is expected to apply to other biomolecules or their

mixtures. Furthermore, the adsorption/desorption processes can be repeated in cycles by a simple change of ionic strength, and the extent of adsorption/desorption can be finely tuned by adjusting the brush composition. In addition to their significance to basic science, these results have practical implications, such as for the development of new biointerfaces for biosensing, separation technologies or nanotransport applications.

ASSOCIATED CONTENT

Supporting Information

This material includes: (i) computations aiming at evaluating: the grafted polymer layers composition, the polymer conformation (brush regime), the thickness of the polymer layers, (ii) AFM images of the brushes formed on gold, (iii) representative QCM-D graphs.

AUTHORS INFORMATION

*Corresponding authors:
christine.dupont@uclouvain.be
ncbratek@cyf-kr.edu.pl

CONFLICT OF INTEREST

The authors confirm that this article content has no conflicts of interest.

ACKNOWLEDGEMENTS

This project has received funding from the European Union's Horizon 2020 research and innovation programme under the Marie Skłodowska-Curie grant agreement No 659391, from the Belgian National Fund for Scientific Research (FNRS), and from BELSPO (Interuniversity Attraction Pole program – P07/05).

REFERENCES

(1) Michael, R; Dorinel, V.; Stefan, S.; Understanding protein adsorption phenomena at solid surfaces" *Adv. Colloid Interface Sci.*, **2011**, *162*, 1–2, 87–106.

(2) Mahon, E.; Salvati, A.; Baldelli Bombelli, F.; Lynch, I.; Dawson, K. A. Designing the nanoparticle-biomolecule interface for targeting and therapeutic delivery, *J. Controlled Release* **2012**, *161*, 164−174.

(3) Kalasin, S.; Santore,M.M.; Non-Specific Adhesion on Biomaterial Surfaces Driven by Small Amounts of Protein Adsorption, *Colloids Surf. B*, **2009**, *73*, p. 229-236.

(4) Brash, J.L.; Horbett, T.A. Proteins at Interfaces: An Over-view. In Proteins at Interfaces II: Fundamentals and Applications; Horbett, T.A., Brash, J.L., Eds.; ACS Symposium Series 602, American Chemical Society: Washington, DC, **1995**; 1 – 23.

(5) Dimilla, P.A.; Albelda, S.M. ; Quin, J.A., Adsorption and elution of extracellular matrix proteins on non-tissue culture polystyrene Petri dishes, *J. Colloid Interface Sci.,* **1992**, *153*, p. 212.

(6) Haynes C.A.; Norde W.; Globular proteins at solid/liquid interfaces. *Colloids Surf., B*, **1994**, *2*, 517–566.

(7) Uhlmann, P.; Ionov, L.; Houbenov, N.; Nitschke, M.; Grundke, K.; Motornov, M.; Minko, S.; Stamm, M., Surface functionalization by smart coatings: Stimuli-responsive binary polymer brushes, *Progress in Organic Coatings,* **2006**, *55*, 168-174 .

(8) Trotsenko, O.; Roiter, Y.; Minko, S. Conformational transitions of flexible hydrophobic polyelectrolytes in solutions of monovalent and multivalent salts and their mixtures, *Langmuir*, **2012**, *28*, 14, 6037-6044.

(9) Currie, E. P. K.; Sieval, A. B.; Fleer, G. J.; Cohen Stuart, M. A., Polyacrylic acid brushes: surface pressure and salt-induced swelling, *Langmuir,* **2000**, *16*, 22, 8324-8333.

(10) Dukhin, S.S.; Zimmermann, R.; Werner, C., Surface conductivity reveals counterion condensation within grafted polyelectrolyte layers, *J. Phys. Chem. B*, **2007**, *111*, 979-981.

(11) Ballauff, M.; Borisov, O., Polyelectrolyte brushes, *Curr. Opin. Colloid Interface Sci.,***2006**, *11*, 316-323.

(12) Zhang, H.; Rühe, J., Swelling of poly(methacrylic acid) brushes: influence of monovalent salt in the environment, *Macromolecules,* **2005,** *38*, 4855-4860.

(13) Czeslik, C.; Jackler, G.; Hazlett, T.; Gratton, E.; Steitz, R.; Wittemann, C. A.; Ballauff, M., Salt-induced protein resistance of polyelectrolyte brushes studied using fluorescence

correlation spectroscopy and neutron reflectometry, *Phys. Chem. Chem. Phys.*, **2004**, *24*, 6, 5557-5563.

(14) Becker, A. L.; Henzler, K.; Welsch, N.; Ballauff, M.; Borisov, O. Proteins and polyelectrolytes: a charged relationship, *Curr. Opin. Colloid Interface Sci.,* **2012**, *17*, (2), 90−96.

(15) Leermakers, F. A. M.; Ballauff, M.; Borisov, O. V. On the mechanism of uptake of globular proteins by polyelectrolyte brushes: A two gradient self-consistent field analysis, *Langmuir*, **2007**, *23* (7), 3937−3946.

(16) Haupt T.; Neumann, A.; Wittemann; Ballauff, M., Activity of enzymes immobilized in colloidal spherical polyelectrolyte brushes, *Biomacromolecules*, **2005**, *6*, 948-955.

(17) Zhang, F.; Kang, E.T.; Neoh, K.G.; Wang, P.; Tan, K.L., Surface modification of stainless steel by grafting of poly (ethylene glycol) for reduction in protein adsorption, *Biomaterials*, **2001**, *22*, 1541-1548.

(18) Wei, J.; Ravn, D.B.; Gram, L.; Kingshott, P., Stainless steel modified with PEG can prevent protein adsorption but not bacterial adhesion, *Colloids Surf. B,* **2005***, 32*, 275-291.

(19) Kingshott, P.; Jiang, W.;Nikolaj G.B.; Lone, G.G., Covalent attachment of poly(ethylene glycol) to surfaces, critical for bacterial adhesion, *Langmuir*, **2001**, *19*, 6912-6921.

(20) Archambault, J.G.; Brash, J.L., Protein repellent polyurethane-urea surfaces by chemical grafting of hydroxyl-terminated poly(ethylene oxide): effects of protein size and charge, 2004, *Colloids Surf. B,* **2004**, *33,* 111-120.

(21) Roosjen, A.; Mei, H.C.; Busscher, H.J.; Norde, W., Microbial adhesion to poly(ethylene oxide) brushes: influence of polymer chain length and temperature", *Langmuir*, **2004**, *20*, 10949-10955.

(22) Unsworth, L.D.; Sheardown H.; Brash, J.L., Protein resistance of surfaces prepared by sorption of end-thiolated poly(ethylene glycol) gold: Effect of surface chain density, *Langmuir*, **2005**, *21*, 1036-1041.

(23) Zheng, J.; Lingyan,L.; Tsao, H.K.;Sheng,Y.J.; Chen,S.; Jiang,S., Strong repulsive forces between protein and oligo(ethylene glycol) self-assembled monolayers. A molecular simulation study, *Biophysical Journal*, **2005**, *89*, (1) 158-166.

(24) Advincula, R.C.; Brittain, W.J.; Caster, K. C.; Ruhe, J., Polymer brushes, Wiley. Online Library, **2004**.

(25) Aulich, D.; Hoy, O.; Luzinov, I.; Brücher, M.; Hergenröder, R.;Bittrich, E.; Eichhorn, K.-J.; Uhlmann, P.; Stamm, M.; Esser, N.;Hinrichs, K., In situ studies on the switching behavior of ultrathin poly(acrylic acid) polyelectrolyte brushes in different aqueous environments, *Langmuir,* **2010**, *26* (15), 12926−12932.

(26) Uhlmann, P.; Houbenov, N.; Brenner, N.; Grundke, K.; Burkert, S.; Stamm, M. In-situ investigation of the adsorption of globular model proteins on stimuli-responsive binary polyelectrolyte brushes. *Langmuir*, **2007**, *23* (1), 57−64.

(27) Hoy, O.; Zdyrko, B.; Lupitskyy, R.; Sheparovych, R.; Aulich, D.;Wang, J. F.; Bittrich, E.; Eichhorn, K. J.; Uhlmann, P.; Hinrichs, K.;Muller, M.; Stamm, M.; Minko, S.; Luzinov, I., Synthetic hydrophilic materials with tunable strength and a range of hydrophobic interactions, *Adv. Funct. Mater.,* **2010**, 20 (14), 2240−2247.

(28) Ionov L.; Minko S.; Stamm M.; Gohy J. F.; Jerome R.; Scholl A., Reversible chemical patterning on stimuli-responsive polymer film: Environment-responsive lithography, *J. Am. Chem. Soc.* **2003**, *125*, 8302-8306.

(29) Ionov L.; Stamm M.; Minko S.; Hoffmann F.; Wolff T., Structuring of Binary Reactive Polymer Brush Layers, *Macromol. Symp.,* **2004,** *207*, 229-236.

(30) Xue C.; Yonet-Tanyeri N.; Brouette N.; Sferrazza M.; Braun P.V.; Leckband D.E., Protein adsorption on poly (N-isopropyl acrylamide) brushes: dependence on grafting density and chain collapse, *Langmuir*, **2011**, *27*, 8810–8818.

(31) Uhlmann, P.; Houbenov, N.; Brenner, N.; Grundke, K.; Burkert, S.; Stamm, M., In-Situ Investigation of the Adsorption of Globular Model Proteins on Stimuli-Responsive Binary Polyelectrolyte Brushes, *Langmuir*, **2007**, *23*(11), 57-64.

(32) Delcroix, M.F.; Huet, G.L.; Conard, T., Demoustier-Champagne, S.; Du Prez F.E.; Landoulsi, J.; Dupont-Gillain, C.C., Design of Mixed PEO/PAA Brushes with Switchable Properties Towards Protein Adsorption, *Biomacromolecules*, **2013**,*14*, 215-225.

(33) Delcroix, M. F.; Demoustier-Champagne, S.; Dupont-Gillain, C.C., Quartz crystal microbalance study of ionic strength and pH-dependent polymer conformation and protein adsorption/desorption on PAA, PEO, and mixed PEO/PAA brushes, *Langmuir,* **2014**, *30*, 268−277.

(34) Delcroix, M.F.; Laurent, S.; Huet, G.L.; Dupont-Gillain, C.C., Protein adsorption can be reversibly switched on and off on mixed PEO/PAA brushes, *Acta Biomaterialia*, **2015**, *11*, 68-79.

(35) Stamm, M.(ed.), Polymer Surfaces and Interfaces, 2008 Springer-Verlag Berlin Heidelberg, p.215-231

(36) Figueira, V.C.; Jones, J.P., Viscoelastic study of the adsorption of bovine serum albumin on gold and its dependence on pH. *J. Colloid Interface Sci*., **2008**, *325*, 107–13.

(37) Carter, D.C.; Ho, J.X., Structure of serum albumin. *Adv. Protein Chem.,* **1994**, *45*, 153–203.

(38) Moulton, S.E.; Barisci, J.N.; Bath, A.; Stella, R.; Wallace, G.G., Investigation of protein adsorption and electrochemical behavior at a gold electrode, *J. Colloid Interface Sci*., **2003**; *261*, 312–319.

(39) Galisteo F, Norde W. Adsorption of lysozyme and α-lactalbumin on poly(styrenesulphonate) lattices. 2. Proton titrations, *Colloids Surf. B*, **1995**, *4*, 389–400.

(40) van der Veen M.; Norde, W.; Stuart, M.C., Electrostatic interactions in protein adsorption probed by comparing lysozyme and succinylated lysozyme, *Colloids Surf. B*, **2004**, *35*, 33–40.

(41) Hollmann O, Czeslik C. Characterization of a planar poly(acrylic acid) brush as a materials coating for controlled protein immobilization, *Langmuir*, **2006**, *22*, 3300–3305.

(42) Wasilewska, M.; Adamczyk, Z.; Jachimska B.; Structure of fibrinogen in electrolyte solutions derived from dynamic light scattering (DLS) and viscosity measurements, *Langmuir*, **2009**, *25*, 3698-3704

(43) Bratek-Skicki, A.; Żeliszewska, P.; Adamczyk, Z., Human fibrinogen adsorption on latex particles at pH 7.4 studied by electrophoretic mobility and AFM measurements, *Curr. Top. Med. Chem.*, **2014**, *14*, 640-648.

(44) Bratek-Skicki,A.; Żeliszewska,P.; Adamczyk, Z., Tuning conformation of fibrinogen monolayers on latex particles by pH of adsorption, *Colloids Surf. B.*, **2013**, *103*, 482-488.

(45) Adamczyk, Z.; Bratek-Skicki, A.; Żeliszewska, P., Mechanisms of fibrinogen adsorption at solid substrates, *Curr. Top. Med. Chem.*, **2014**, *14*, 702-709.

(46) Psarra E.; König U.; Ueda Y. ; Bellmann C.; Janke A.; Bittrich E.; Eichhorn K.J.; Uhlmann P., Nanostructured biointerfaces: nanoarchitectonics of thermoresponsive polymer brushes impact protein adsorption and cell adhesion, *ACS Appl. Mater. Interfaces*, **2015**, *17*, 7 (23):12516-29.

(47) Zor, T.; Selinger, Z., Linearization of the Bradford protein assay increases its sensitivity: theoretical and experimental studies, *Anal. Biochem*., **1996**, *236* (2), 302-308.

(48) Reviakine,I.; Johannsmann, D.; Richter, R.P., Hearing what you cannot see and visualizing what you hear; Interpreting quartz crystal microbalance data from solvated interfaces, *Anal. Chem.*, **2011**, *83*, 23, p. 8838-8848.

(49) Adamczyk, Z.; Bratek, A.; Szelag, E.; Bastrzyk, A.; Michna, A.;Barbasz, J., Colloid particle deposition on heterogenous surfaces produced by polyelectrolyte adsorption, *Colloids Surf. A*., **2009**, *343*, 111-117.

(50) Morga, M.; Adamczyk, Z. Monolayers of cationic polyelectrolytes on mica - Electrokinetic studies, *J. Colloid Interface Sci*., **2013**, *407*, 196-204.

(51) Brandrup, J.; Immergut, E.H.; Grulke, E.A., Polymer Handbook, **1999**, Hoboken, New Jersey: John Wiley&Sons. 2336.

(52) Giesbers, M.; Kleijn, J.M.; Stuart, M.A, The electrical double layer on gold probed by electrokinetic and surface force measurements, *J Colloid Interface Sci*., **2002**, *248*(1), 88-95.

(53)Jachimska B.; Kozlowska A.; Pajor-Swierzy, A., Protonation of lysozyme and its consequences for the adsorption onto a mica surface, *Langmuir*, **2012**, 28 (31), 11502–11510.

(54) Morga,M;. Michna, A.; Adamczyk, Z., Formation and stability of polyelectrolyte/polypeptide monolayers determined by electrokinetic measurements, *Colloids Surf. A*., **2017***, 529,* 302-310.

(55) Morga,M.; Adamczyk,Z.; Gödrich,S.; Oćwieja, M.; Papastavrou, G., Monolayers of poly-L-lysine on mica – Electrokinetic characteristics. *J. Colloid Interface Sci*., **2015***, 456,* 116-124.

(56) Dąbkowska, M.; Z. Adamczyk, Z., Human serum albumin monolayers on Mica: Electrokinetic characteristics, *Langmuir,* **2012***, 28,* 15663-15673.

(57) Żeliszewska, P.; Bratek-Skicki, A.; Adamczyk, Z.; Ciesla, M., Modelling and measurements of fibrinogen adsorption on positively charged microspheres, *Cond. Mat. Phys.* **2016**, *19*, 1-14.

(58) Wasilewska, M.; Adamczyk, Z., Fibrinogen adsorption on mica studied by AFM and in situ streaming potential measurements, *Langmuir,* **2011**, *27,* 686-696.

(59) Yigit, C.; Kanduc, M. ; Ballau, M.; Dzubiella, J., Interaction of Charged Patchy Protein Models with Like-Charged Polyelectrolyte Brushes, *Langmuir*, **2017**, *33*, 417-442.

(60) Wittemann, A.; Haupt ,B.; Ballauff M., Controlled Release of Proteins Bound to Spherical Polyelectrolyte Brushes, *Zeitschrift für Physikalische Chemie*, **2007**, *221*, 113-126.

(61) Jung, S.Y.; Lim, S.M.; Albertorio, F.; Kim, G.; Marc C. G.; Yang, R. D.; Holden, M. A.; Cremer, P. S., The Vroman Effect: A molecular level description of fibrinogen displacement. *J. Am. Chem. Soc.,* **2003**, *125,* 12782-12786.

(62) Jachimska, B.; Wasilewska, M.; Z.Adamczyk, Z., Characterization of globular protein solutions by dynamic light scattering, electrophoretic mobility, and viscosity measurements, *Langmuir*, **2008**, *24*, 6866-6872.

(63)Psarra, E., Biofunctionalization of polymer brush surfaces, PhD thesis, **2015**, p. 91.

(64) Belegrinou, S.; Mannelli, I.; Lisboa, P.; Bretagnol, F.; Valsesia, A.; Ceccone, G.; Colpo, P.; Rauscher, H.; Rossi, F. pH-dependent immobilization of proteins on surfaces functionalized by plasma- enhanced chemical vapor deposition of poly(acrylic acid)- and poly(ethylene oxide)-like films. *Langmuir*, **2008**, *24*, 7251−7261.

TOC